

# Towards Hybrid Bronchoscope Tracking under Respiratory Motion - Evaluation on a Dynamic Motion Phantom

Xióngbiāo Luó<sup>a</sup>, Marco Feuerstein<sup>a</sup>, Takamasa Sugiura<sup>a</sup>,  
Takayuki Kitasaka<sup>b,c</sup>, Kazuyoshi Imaizumi<sup>c,d</sup>, Yoshinori Hasegawa<sup>c,d</sup>, Kensaku Mori<sup>e,a,c</sup>

<sup>a</sup>Graduate School of Information Science, Nagoya University, Japan;

<sup>b</sup>Faculty of Information Science, Aichi Institute of Technology, Japan;

<sup>c</sup>MEXT Innovation Center for Preventive Medical Engineering, Nagoya University, Japan;

<sup>d</sup>Graduate School of Medicine, Nagoya University, Japan;

<sup>e</sup>Information Planning Office, Information and Communications Headquarters,  
Nagoya University, Japan

## ABSTRACT

This paper presents a hybrid camera tracking method that uses electromagnetic (EM) tracking and intensity-based image registration and its evaluation on a dynamic motion phantom. As respiratory motion can significantly affect rigid registration of the EM tracking and CT coordinate systems, a standard tracking approach that initializes intensity-based image registration with absolute pose data acquired by EM tracking will fail when the initial camera pose is too far from the actual pose. We here propose two new schemes to address this problem. Both of these schemes intelligently combine absolute pose data from EM tracking with relative motion data combined from EM tracking and intensity-based image registration. These schemes significantly improve the overall camera tracking performance. We constructed a dynamic phantom simulating the respiratory motion of the airways to evaluate these schemes. Our experimental results demonstrate that these schemes can track a bronchoscope more accurately and robustly than our previously proposed method even when maximum simulated respiratory motion reaches 24 mm.

**Keywords:** Hybrid Bronchoscope Tracking, Intensity-based Image Registration, Dynamic Motion Phantom

## 1. INTRODUCTION

Lung and bronchus cancer is the leading cause of cancer death in the United States. In 2009, 219440 new cases were diagnosed, accounting for about 15 percent of total cancer diagnoses.<sup>1</sup> It is desirable to diagnose cancer as early as possible, so physicians can remove tumor tissue at its early stage. However, it can be difficult to navigate the bronchoscope and biopsy needles to suspicious tissue, in particular in the peripheral airways where the airway tree is complex. Therefore, navigated bronchoscopy was proposed to help a physician to diagnose and treat lung and bronchus cancer. Navigated bronchoscopy provides various kinds of navigation information, such as locations of abnormal regions, paths to abnormal regions where the biopsy needs to be performed, anatomical names of

---

Further author information: (Send correspondence to X. L.)

X. L.: E-mail: xbluo@suenaga.m.is.nagoya-u.ac.jp, Telephone: +81 52 789 5688

M. F.: E-mail: fmarco@suenaga.m.is.nagoya-u.ac.jp

T. K.: E-mail: kitasaka@aitech.ac.jp

K. M.: E-mail: kensaku@is.nagoya-u.ac.jp

---

Copyright 2010 Society of Photo-Optical Instrumentation Engineers.

This paper was published in SPIE Medical Imaging and is made available as an electronic reprint with permission of SPIE. One print or electronic copy may be made for personal use only. Systematic or multiple reproduction, distribution to multiple locations via electronic or other means, duplication of any material in this paper for a fee or for commercial purposes, or modification of the content of the paper are prohibited.

currently displayed branches, and in particular visualization of anatomical structures beyond bronchial walls. All of this information is provided relative to the current pose (position and orientation) of the bronchoscope.

To obtain the bronchoscope pose, a tracking method based on image registration or EM tracking (or a combination of both) is usually used in bronchoscopic navigation systems. Many papers have been published on this topic.<sup>2-8</sup> Higgins et al. proposed a method for bronchoscope tracking using intensity-based image registration utilizing normalized mutual information.<sup>9</sup> Its tracking speed and accuracy was improved by employing 2D/2D matching frameworks to obtain the 3D camera motion.<sup>5</sup> Deligianni et al. proposed bronchoscope tracking using a position sensor and a  $pq$ -based registration technique. This tracking method yielded more accuracy and stability by modeling the respiratory motion with an active shape model.<sup>4</sup> It tries to generate virtual bronchoscopic (VB) images that are as similar as possible to real bronchoscopic (RB) images by recovering a bidirectional reflectance distribution function (BRDF) from registered RB and VB images.<sup>10</sup> Our group uses optical flow patterns to compute bronchoscope motion between consecutive RB images as a pre-registration step for bronchoscopic navigation.<sup>3</sup> We also improved registration performance in bronchoscope tracking by only selecting meaningful image regions.<sup>11</sup>

Regardless of which bronchoscopic guidance method is used, bronchoscope tracking is a key component in the development of such a guidance system. It is desirable to precisely track the movements of the camera at the tip of the bronchoscope. Unfortunately, it is still difficult to accurately track bronchoscope movement since intensity-based image registration-based methods are often affected by problematic bronchoscopic video frames (e.g. bubbles or the bronchoscope looking onto the bronchial wall.) Also EM tracking is sensitive to patient movement such as respiratory motion or coughing.

This paper presents a method for more accurate and robust bronchoscope tracking. We propose a hybrid camera tracking method that intelligently combines EM tracking and intensity-based image registration. Hybrid bronchoscope tracking uses the results of EM tracking to initialize the optimization task during image registration. To improve the accuracy and robustness of hybrid bronchoscope tracking, we use a flexible scheme of initialization of intensity-based image registration. We also employ hand-eye calibration to compute the transformation between sensor and camera coordinate systems. We evaluated our proposed method on a dynamic phantom simulating the motion of the airways.

The remainder of this paper is organized as follows. We define all necessary coordinate systems and transformations and outline our proposed hybrid bronchoscope tracking method in Section 2. Section 3 shows the experimental environment and the results of the proposed method. Finally, Section 4 discusses the results of the proposed method, before concluding this work in Section 5.

## 2. METHOD

Hybrid bronchoscope tracking initializes image registration by the EM tracking-based result. The problem in hybrid bronchoscope tracking is how to use EM tracker outputs for initialization of image registration for bronchoscope pose estimation under respiratory motion. We address this initialization problem by choosing either absolute or relative EM tracking measurements to initialize the image registration: (a) absolute: transform the camera pose from EM coordinate system to CT coordinate system, (b) relative: multiply the pose offset between the last and the current frame onto the camera pose resulting from the registration of the last frame.

Generally, our proposed hybrid bronchoscope tracking method comprises three stages: (a) camera and hand-eye calibration. We apply camera calibration to obtain the intrinsic parameters of the bronchoscope camera and employ hand-eye calibration to perform the EM sensor and camera alignment. (b) CT-to-physical space registration. This step is performed to obtain the initial rigid registration between EM and CT tracking coordinate systems. We can use a landmark-based or a landmark-free method to calculate this transformation.<sup>12,13</sup> (c) initialization of image registration. For each bronchoscopic video frame, our method combines EM tracking with intensity-based image registration to perform camera tracking, where the latter maximizes images similarities between RB and VB images generated by volume rendering to achieve good intensity-based image registration.<sup>11</sup> The main point of this stage is to choose the initialization of the image registration. Additionally, we use a dynamic phantom to simulate the respiratory motion for evaluating the performance of our hybrid tracking method.

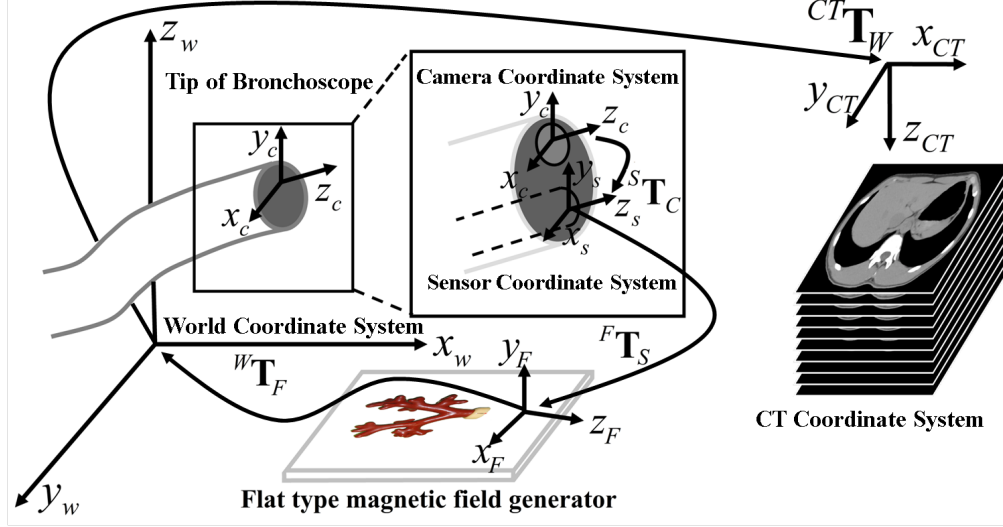


Figure 1: Relationship between coordinate system in our bronchoscopic navigation.

Since we use an EM tracking system in our method, we must define the coordinate systems we will use. Figure 1 presents an outline of the relationships and transformation matrices between each coordinate system. As shown in Figure 1,  ${}^F\mathbf{T}_S$  describes the relationship between the sensor coordinate system and the magnetic field coordinate system.  ${}^W\mathbf{T}_F$  is from the magnetic field coordinate system to the world coordinate system, and  ${}^{CT}\mathbf{T}_W$  is from the world coordinate system to the CT coordinate system. We formulate the relationship between the sensor coordinate system and the world coordinate system as  ${}^W\mathbf{T}_S^{(i)} = {}^W\mathbf{T}_F {}^F\mathbf{T}_S^{(i)}$ , where  ${}^F\mathbf{T}_S^{(i)}$  is the  $i$ -th EM sensor output. Additionally, the transformation between the camera and the sensor (both attached at the tip of the bronchoscope) is represented by  ${}^S\mathbf{T}_C$ .

## 2.1 Camera and Hand-Eye Calibration

We must calculate the rigid transformation matrix  ${}^S\mathbf{T}_C$  between the bronchoscope camera and the EM sensor coordinate systems. For that, we utilize hand-eye calibration. This technique was introduced for a variety of robotic applications. It computes the spatial relationship from the hand (e.g. a robot gripper) to the eye (e.g. a camera) that is an unknown rigid transformation which can be determined from a number of acquired camera and gripper motions. In our situation, the “hand” corresponds to the EM sensor while the “eye” relates to the bronchoscope camera. We here utilize the hand-eye calibration method to calculate the transformation between the EM sensor coordinate system and the camera coordinate system by

$$\Delta^S\mathbf{T}_{ij} {}^S\mathbf{T}_C = {}^S\mathbf{T}_C \Delta^C\mathbf{T}_{ij} \quad (1)$$

where  $\Delta^S\mathbf{T}_{ij}$  is the sensor movement relative to the EM tracker coordinate system  $\Delta^S\mathbf{T}_{ij} = {}^S\mathbf{T}_F^{(i)} {}^F\mathbf{T}_S^{(j)}$ , and  $\Delta^C\mathbf{T}_{ij}$  is the camera motion relative to a calibration pattern frame  $\Delta^C\mathbf{T}_{ij} = {}^C\mathbf{T}_P^{(i)} {}^P\mathbf{T}_C^{(j)}$ , for the bronchoscope performing a movement from the  $i$ -th pose to the  $j$ -th pose. Equation 1 can be directly obtained from Figure 2.

During hand-eye calibration we first acquire pairs of calibration pattern<sup>14</sup> images and EM sensor outputs. We next perform a calibration of the intrinsic and distortion parameters of the bronchoscope camera and estimate the camera pose  ${}^C\mathbf{T}_P^{(i)}$  for each frame  $i$  utilizing Zhang’s method.<sup>15</sup> Then, we solve Equation 1 to obtain the transformation  ${}^S\mathbf{T}_C$ .<sup>16</sup>

After hand-eye calibration, we calculate an initial transformation from the world (patient) coordinate system to the CT coordinate system by localizing corresponding points in the EM tracking and CT coordinate system and computing the rigid transformation between the two point clouds<sup>17</sup> as outlined in the next section.

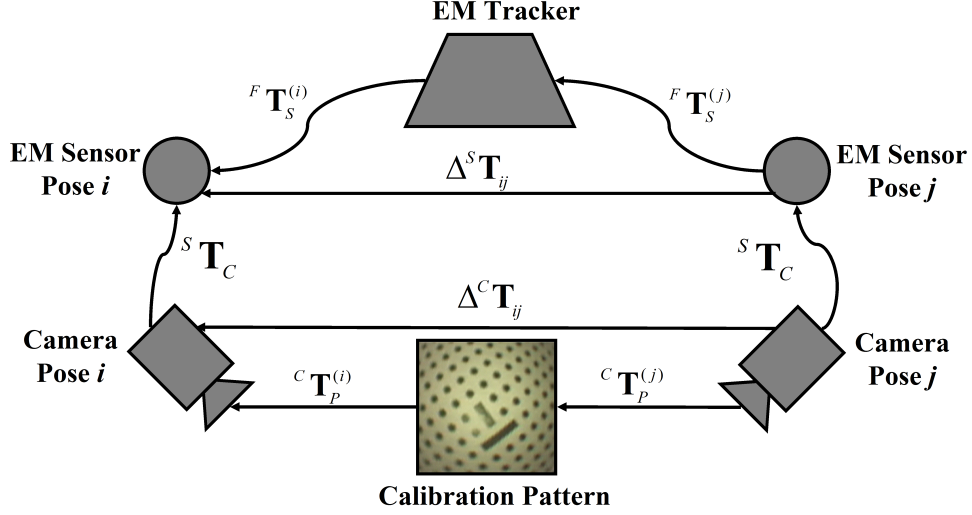


Figure 2: Hand-eye calibration setup from camera pose estimation and EM sensor outputs.

## 2.2 CT-to-Physical Space Registration

For EM tracking, it is required to estimate the mapping between the world coordinate system and the CT coordinate system. This transformation  ${}^{CT}\mathbf{T}_W$  is calculated using point-based registration.

In the bronchoscopy room, practical approaches need to be chosen to obtain this transformation  ${}^{CT}\mathbf{T}_W$  when using an EM tracking system, such as the commercially available superDimension navigation system.<sup>12, 18</sup> Either external or internal landmarks are usually used to estimate  ${}^{CT}\mathbf{T}_W$ . While external landmarks are commonly fiducials attached to the patient skin before CT acquisition, internal landmarks are usually natural landmarks such as the carina and bifurcations. No matter what landmarks are utilized, they should be designed to be clearly identifiable in both CT and the patient's body. By localizing the two sets of points (the positions of the landmarks) in the world coordinate system and the CT coordinate system, we can calculate  ${}^{CT}\mathbf{T}_W$  by using point-based registration.<sup>17</sup>

For landmark-based rigid registration, we use the positional sensor to measure external or internal landmarks and acquire a series of outputs  $(\mathbf{p}_W^1, \dots, \mathbf{p}_W^n)$  related to the bronchoscope position. After that, we computed the transformation  ${}^{CT}\mathbf{T}_W$  between the EM sensor outputs  $(\mathbf{p}_W^1, \dots, \mathbf{p}_W^n)$  and the corresponding positions  $(\mathbf{p}_{CT}^1, \dots, \mathbf{p}_{CT}^n)$  measured manually in the CT coordinate system by minimizing the registration error<sup>17</sup>

$$Err = \frac{1}{n} \sum_{i=1}^n \|\mathbf{p}_{CT}^i - {}^{CT}\mathbf{T}_W \mathbf{p}_W^i\|. \quad (2)$$

Alternatively, we can also use a landmarks-free method<sup>13</sup> to calculate  ${}^{CT}\mathbf{T}_W$ , which matches the centerline of the bronchial tree and EM sensor output to obtain this transformation.

## 2.3 Initialization of Image Registration

From the  $i$ -th output  ${}^W\mathbf{T}_S^{(i)}$  of the EM sensor  $S$  inside the working channel of the bronchoscope, we can calculate an initial transformation from the camera coordinate system to the CT coordinate system by

$${}^{CT}\mathbf{T}_C^{(i)} = {}^{CT}\mathbf{T}_W {}^W\mathbf{T}_S^{(i)} S \mathbf{T}_C \quad (3)$$

where  ${}^{CT}\mathbf{T}_W$  is the mapping between the world coordinate system and the CT coordinate system, and  $S \mathbf{T}_C$  is the transformation between the sensor coordinate system and the camera coordinate system; they were previously computed by the rigid CT-to-physical space registration and the hand-eye calibration, respectively.

However, as respiratory motion significantly affects the accuracy of this rigid registration and hence the initialization quality of intensity-based image registration, we propose two new schemes to refine the registration.

### 2.3.1 Respiration Sensor-Based Refinement (Method 1)

Our first scheme uses an additional EM sensor for estimating the current phase of the breathing motion, so we have one sensor ( $S$ ) inserted into the working channel of the bronchoscope and another one ( $S^*$ ) attached to the moving airway phantom, which would be placed on the patient’s chest wall in the bronchoscopy suite. We now modify the initialization by using the output of sensor  $S^*$ . Let the outputs  ${}^W\mathbf{T}_{S^*}^{(i-1)}$  and  ${}^W\mathbf{T}_{S^*}^{(i)}$  of sensor  $S^*$  correspond to the outputs  ${}^W\mathbf{T}_S^{(i-1)}$  and  ${}^W\mathbf{T}_S^{(i)}$  of sensor  $S$  when recording the  $(i-1)$ -th RB image and the  $i$ -th RB image. The initial transformations  ${}^{CT}\mathbf{T}_C^{(i-1)}$  and  ${}^{CT}\mathbf{T}_C^{(i)}$  are calculated by Eq. 3. Depending on the phase information from sensor  $S^*$ , we modify the initialization of intensity-based image registration.

We compute the Euclidean distance  $d_i$  between the current position of the sensor  $S^*$  and the position of  $S^*$  corresponding to the phase in which the CT was acquired (usually either inspiration or expiration). Then we check whether this distance is greater than a threshold  $t$  (e.g., set to the minimum radius of the airways) or not. If it is greater than this threshold, we assume that the tracking measurements transformed into the CT coordinate system will lie outside the airways. Therefore, for refining the registration procedure, we use

- Either the original absolute EM tracking result  ${}^{CT}\mathbf{T}_C^{(i)}$  to initialize intensity-based image registration, if we are in a phase similar to the one in which the CT was acquired, i.e. when  $d_i \leq t$ .
- Or compute the relative EM sensor output (transformation)  $\Delta^W\mathbf{T}_C = {}^W\mathbf{T}_C^{(i)}({}^W\mathbf{T}_C^{(i-1)})^{-1}$  between the last frame and the current frame and transformation into the CT coordinate system  $\Delta{}^{CT}\mathbf{T}_C$  by Eq. 3, and then multiplication of  $\Delta{}^{CT}\mathbf{T}_C$  onto the result of the last registration (instead of using the absolute EM tracking measurement) to initialize intensity-based image registration, if we are too far from the phase in which the CT was acquired, i.e. when  $d_i > t$ .

### 2.3.2 Image Similarity-Based Refinement (Method 2)

Our second scheme decides on the image similarity between RB and VB images whether to use a absolute or a relative transformation. It is not dependent on any information about the respiratory phase, so we do not require an additional EM tracking sensor or a previous determination of a suitable threshold. We perform the initial rigid registration in the same way as for the first scheme. However, instead of deciding whether to use absolute or relative transformations before intensity-based image registration, we perform intensity-based image registration once initialized with absolute sensor pose information and once with a relative sensor transformation multiplied onto the last tracking result and decide on the resulting image similarities which registration result is finally used. In detail, for tracking each frame we perform the following steps:

- **Step 1:** Execution of intensity-based image registration initialized by an absolute EM sensor measurement and computation of the final image similarity  $D_1$ .
- **Step 2:** Execution of intensity-based image registration initialized by the relative EM sensor output (transformation)  $\Delta^W\mathbf{T}_C = {}^W\mathbf{T}_C^{(i)}({}^W\mathbf{T}_C^{(i-1)})^{-1}$  between the last frame and the current frame and transformation into the CT coordinate system  $\Delta{}^{CT}\mathbf{T}_C$  by Eq. 3, and then multiplication of  $\Delta{}^{CT}\mathbf{T}_C$  onto the result of the last registration and calculation of the final image similarity  $D_2$ .
- **Step 3:** Comparison of the similarities  $D_1$  and  $D_2$ . If  $D_1 > D_2$ , we choose the tracking result corresponding to  $D_1$ , otherwise we take the result corresponding to  $D_2$ .

## 3. EXPERIMENTAL RESULTS

For evaluating the performance of the proposed tracking method, we manufactured a dynamic bronchial phantom (see Figure 3) for simulating breathing motion. We connect the rubber phantom to a motor by using a nylon thread. A LEGO Mindstorm (LEGO, Denmark) is utilized as power source to generate movements. Utilizing the controller part (the NXT: a programmable robotics kit included in the LEGO Mindstorm), we can control the motor motion including direction and rotational speed. The phantom thus simulates respiratory motion when the thread changes its length. Additionally, an EM sensor ( $S^*$ ) is attached on the bronchial surface to

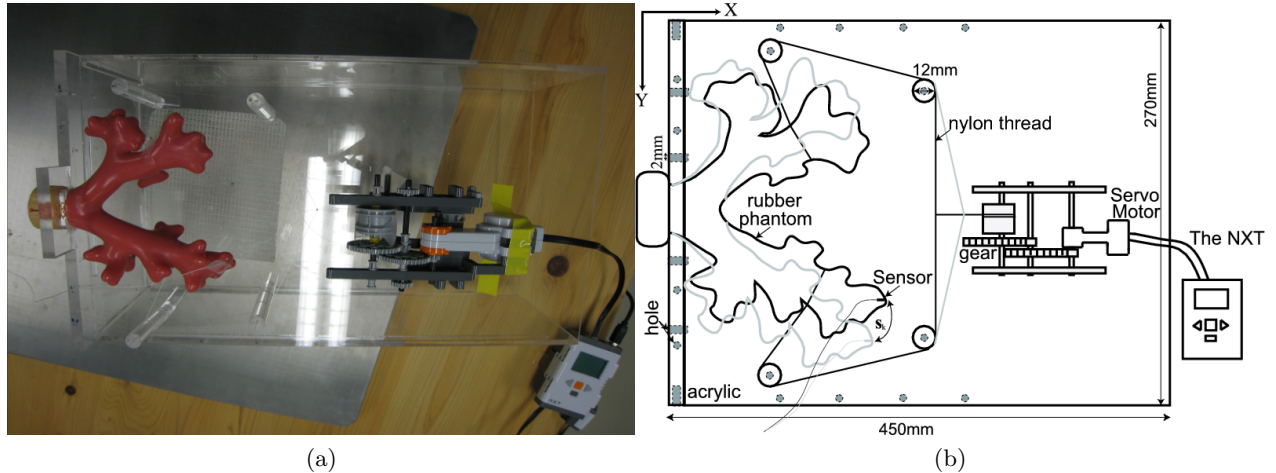


Figure 3: Dynamic motion phantom. (a) Picture of real phantom and (b) Drawing of the phantom movement.

measure the bronchial deformation that we used to choose the current breathing phase. It is possible to adjust the amount of the simulated motion and its maximum is about 24 mm.

To calculate  ${}^{CT}\mathbf{T}_W$  precisely,  $n$  pipes are drilled into the acrylic box where the bronchial phantom is attached on (as shown in Figure 3). Firstly, we inserted the positional sensor into the pipes and acquired a series of outputs ( $\mathbf{p}_W^1, \dots, \mathbf{p}_W^n$ ) related to the bronchoscope position. After that, we computed the transformation  ${}^{CT}\mathbf{T}_W$  between the EM sensor outputs ( $\mathbf{p}_W^1, \dots, \mathbf{p}_W^n$ ) and the corresponding positions ( $\mathbf{p}_{CT}^1, \dots, \mathbf{p}_{CT}^n$ ) measured manually in the CT coordinate system by minimizing the registration error by Eq. 2. Here, ( $\mathbf{p}_W^1, \dots, \mathbf{p}_W^n$ ) are acquired 100 times under fixation of the EM sensor, computing average values. In our experiments, we used 29 pipes ( $n = 29$ ) for computing  ${}^{CT}\mathbf{T}_W$ , and the registration error was about 1.0 mm.

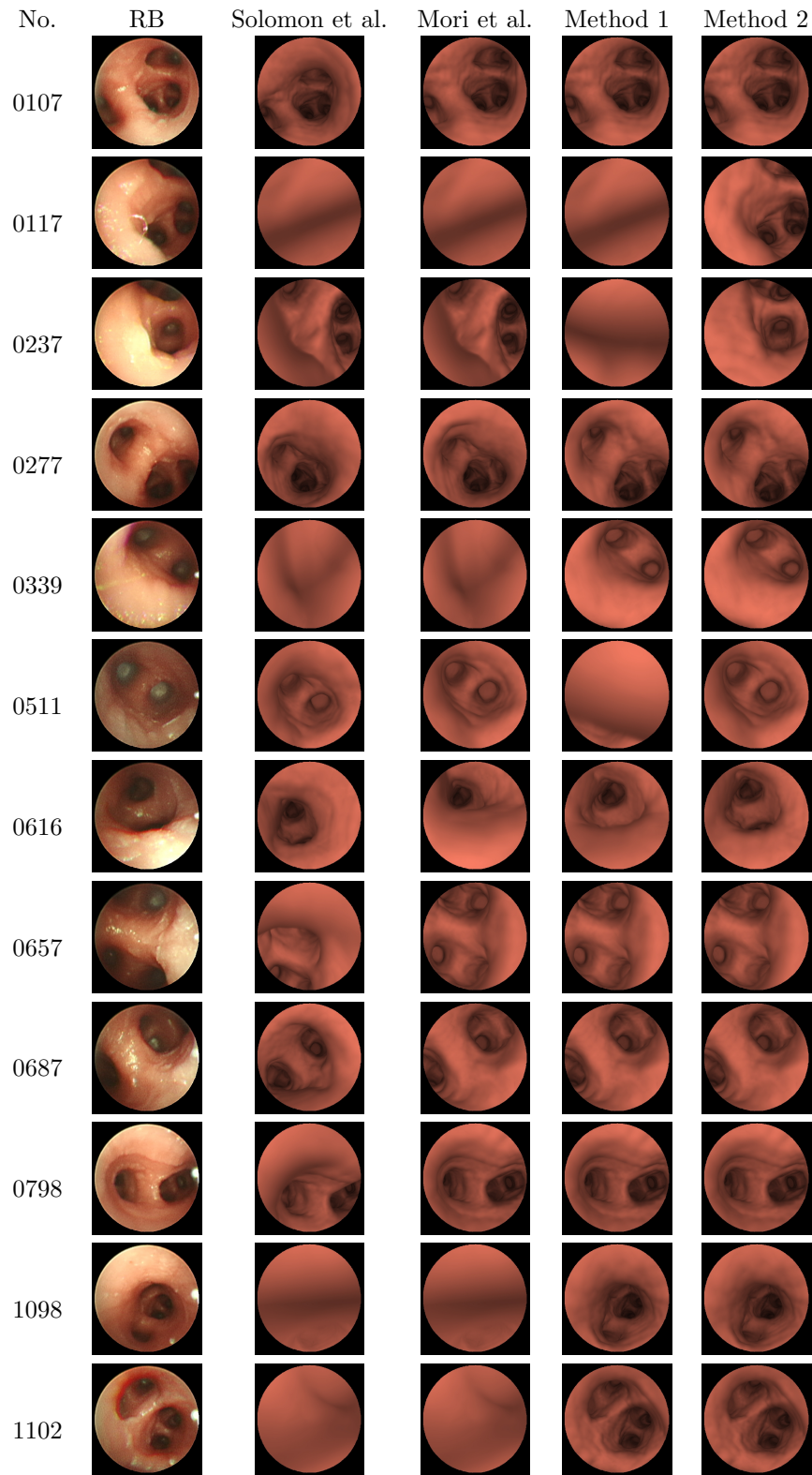
A CT scan of the phantom was acquired according to a standard clinical protocol. The acquisition parameters of the CT images are:  $512 \times 512$  pixels, 1021 slices, 0.5 mm slice thickness, 0.68 mm reconstruction pitch. Bronchoscopic videos were recorded at 30 frames per second. The image size of the video frames is  $362 \times 370$  pixels. We have done all implementations on a Microsoft Visual C++ platform and ran the software on a conventional PC (CPU: Intel XEON 3.80 GHz  $\times$  2 processors, 4-GByte main memory).

In our experiments, we used a 3-D Guidance medSAFE tracker from Ascension Technology Corporation\* for EM tracking. It has a 4-coil flat type transmitter as magnetic field generator. The coil diameter of the EM sensor we used is 1.3 mm and its length is around 6.6 mm. The bronchoscope is of type BF-P260F and manufactured by Olympus. Its diameter is 4.0 mm. We fixed the EM sensor inside the working channel of the bronchoscope during hybrid bronchoscope tracking.

For dynamic phantom validation, we compare four tracking schemes according to: (a) Solomon et al.<sup>12</sup> only using EM tracking, (b) Mori et al.<sup>8</sup> intensity-based image registration directly initialized by the results of EM tracking, (c) Method 1: our first new scheme according to Section 2.3.1, refining the EM-based estimation using a respiration sensor and thresholding the respiratory phase, and (d) Method 2: our second new scheme according to Section 2.3.2, refining the EM-based estimation based on the similarities resulting from intensity-based image registration initialized in two ways.

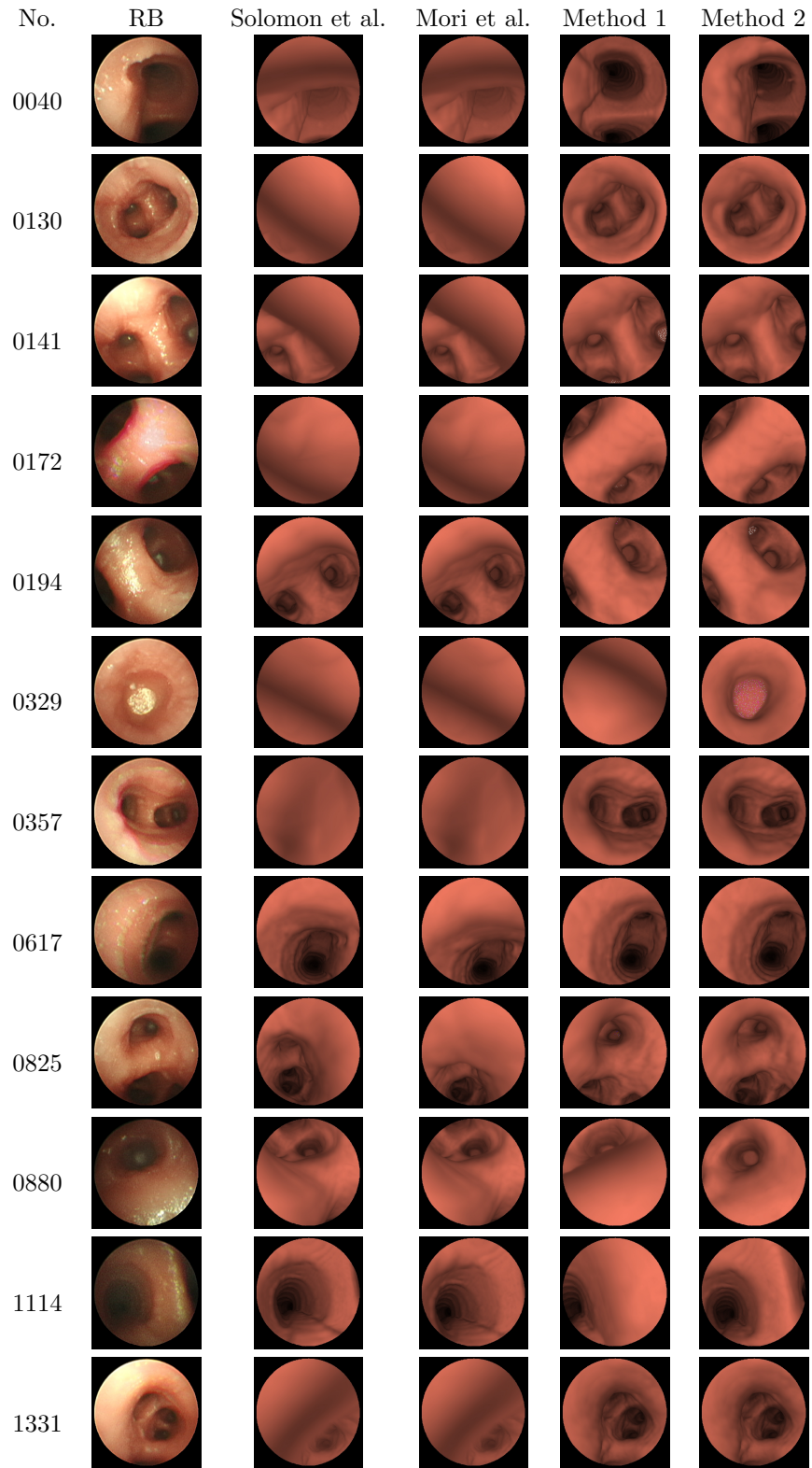
Table 1 shows the quantitative results of the evaluation of the methods. We here count the number of frames that are successfully registered. The maximum simulated respiratory motion for different experiments is also shown in Table 1. As you can see, our proposed Methods 1 and 2 significantly improve the registration performance. Furthermore, examples of experiments B and D for successfully registered frames are displayed in Figure 4. It shows examples of RB images and the corresponding VB images generated from the camera parameters predicted by each method.

\*<http://www.ascension-tech.com/>



(a) Experiment B.

Figure 4: Results of bronchoscope tracking by different methods under simulated breathing motion using our dynamic phantom. The left column shows selected frame numbers of phantom RB images and their corresponding phantom RB images. The other columns display virtual bronchoscopic images generated from the tracking results, comparing our two methods to previous methods. Method 2 shows the best performance compared with other methods.



(a) Experiment D.  
Figure 4: *Continued.*



Table 1: Quantitative comparison of the registered results.

Experiment	Maximum Motion[mm]	Num. of Frames	Number of successfully registered frames			
			Solomon et al <sup>12</sup>	Mori et al <sup>8</sup>	Method 1	Method 2
A	7.25	1245	810 (65.1%)	918 (73.7%)	982 (78.9%)	1076 (86.4%)
B	12.72	1274	731 (57.4%)	811 (63.7%)	905 (71.0%)	1042 (81.8%)
C	19.42	1522	842 (55.3%)	921 (60.5%)	998 (65.6%)	1164 (76.5%)
D	24.33	1445	693 (48.0%)	827 (57.2%)	903 (62.5%)	1015 (70.2%)
<b>Total</b>		<b>5486</b>	<b>3076 (56.1%)</b>	<b>3477 (63.4%)</b>	<b>3708 (67.6%)</b>	<b>4297 (78.3%)</b>

#### 4. DISCUSSION

The objective of this study is to design and improve the performance of hybrid bronchoscope tracking during bronchoscopic navigation. We improve our previously developed hybrid tracking method<sup>8</sup> in various aspects. We utilize two EM sensors to estimate the bronchoscope pose and the current respiratory phase. According to the respiratory phase, we can refine the initialization of intensity-based image registration. Alternatively, we improve the tracking performance by subsequently performing two (differently initialized) intensity-based image registrations and, depending on the resulting image similarity, adapting the tracking result. Additionally, we use hand-eye calibration to enhance the accuracy of the transformation between sensor coordinate and camera coordinate systems. We construct a new dynamic motion phantom of the airways to evaluate our proposed method.

As shown in Table 1 and Figure 4, it is obvious that Method 1 and 2 are more accurate and robust than our previous method,<sup>8</sup> which directly initializes intensity-based image registration with EM tracking. This is because our proposed methods constrain the registration to roughly stay within the airway tree. For Method 1, if the measurements of the phase sensor  $S_2$  are too far from the phase the CT was acquired in, we just replace absolute EM tracking measurements by relative EM measurements. This results in a more accurate initialization of intensity-based image registration and reduces the registration error. However, Method 2 shows even better tracking results. We attribute this to the difficulty of choosing a proper threshold for Method 1. The average runtime of Method 2 per frame (752 ms) is higher than that of Method 1 (343 ms), because we need to perform two intensity-based image registrations.

However, in our experiments, all methods presented here still fail to correctly register all RB and VB frames when continuously tracking the bronchoscope. We believe that this failure is caused by the following problems during hybrid bronchoscope tracking. First, the accuracy of bronchoscope tracking is also affected by the performance of camera and hand-eye calibration and CT-to-physical space registration. We already introduced some error when performing these two stages: (1) the calibration error is about 1.2 mm and (2) the registration error is around 1.0 mm. Next, as the measurement accuracy of EM tracking is affected by magnetic field distortions caused by metals or conductive material within or close to the working volume, the bronchoscope containing ferrous material itself disturbs the measurements. Third, intensity-based image registration depends on characteristic structures such as folds or bifurcations in the bronchial tree of the patient to calculate the camera position corresponding to an RB image,<sup>11</sup> which are not always visible. Finally, our simulated breathing motion is rather big and not realistic enough. Currently it is only in the left-right and superior-inferior directions for the peripheral lung. The trachea is not moving. The magnitude of the motion can be adjusted to 7 ~ 24 mm. However, for a real patient, the respiratory motion is greatest in the superior-inferior direction (~ 9 mm), moderate in the anterior-posterior direction (~ 5 mm), and lowest in the left-right direction (~ 1 mm).<sup>19</sup>

#### 5. CONCLUSIONS

We presented a hybrid camera tracking method using electromagnetic (EM) tracking and intensity-based image registration. We propose flexible schemes for the initialization of intensity-based image registration, intelligently combining absolute and relative EM tracking data with intensity-based image registration to reduce the influence of respiratory motion. The experimental results tested on a dynamic phantom demonstrated that our proposed methods significantly improve the performance of intensity-based image registration by intelligently refining the initial camera pose used for registration.

## ACKNOWLEDGMENTS

This work was supported by the “China Scholarship Council Postgraduate Scholarship Program”, by the JSPS postdoctoral fellowship program for foreign researchers, by the program of formation of innovation center for fusion of advanced technologies “Establishment of early preventing medical treatment based on medical-engineering for analysis and diagnosis” funded by MEXT, by a Grant-in-Aid for Science Research funded by MEXT and JSPS, and by a Grant-in-Aid for Cancer Research funded by the Ministry of Health, Labour and Welfare, Japan.

## REFERENCES

- [1] Jemal, A., Siegel, R., Ward, E., Hao, Y., Xu, J., and Thun, M. J., “Cancer statistics, 2009,” *CA: A Cancer Journal for Clinicians* **59**(4), 225–249 (2009).
- [2] I. Bricault, G. F. and Cinquin, P., “Registration of real and ct-derived virtual bronchoscopic images to assist transbronchial biopsy,” *IEEE Transaction on Medical Imaging* **17**(5), 703–714 (1998).
- [3] Mori, K., Deguchi, D., Sugiyama, J., Suenaga, Y., Toriwaki, J., Jr., C. M., Takabatake, H., and Natori, H., “Tracking of a bronchoscope using epipolar geometry analysis and intensity based image registration of real and virtual endoscopic images,” *Medical Image Analysis* **6**, 321–336 (2002).
- [4] Deligianni, F., Chung, A. J., and Yang, G. Z., “Nonrigid 2-d/3-d registration for patient specific bronchoscopy simulation with statistical shape modeling: Phantom validation,” *IEEE Transactions on Medical Imaging* **25**(11), 1462–1471 (2006).
- [5] Helferty, J., Sherbondy, A., Kiraly, A., and Higgins, W., “Computer-based system for the virtual-endoscopic guidance of bronchoscopy,” *Computer Vision and Image Understanding* **108**, 171–187 (2007).
- [6] Schwarz, Y., Greif, J., Becker, H. D., Ernst, A., and Mehta, A., “Real-time electromagnetic navigation bronchoscopy to peripheral lung lesions using overlaid ct images: the first human study,” *Chest* **129**(4), 988–994 (2006).
- [7] Gildea, T. R., Mazzone, P. J., Karnak, D., Meziane, M., and Mehta, A. C., “Electromagnetic navigation diagnostic bronchoscopy: a prospective study,” *American Journal of Respiratory and Critical Care Medicine* **174**(9), 982–989 (2006).
- [8] Mori, K., Deguchi, D., Akiyama, K., Kitasaka, T., Mauer, C. R. J., Suenaga, Y., Takabatake, H., Mori, M., and Natori, H., “Hybrid bronchoscope tracking using a magnetic tracking sensor and image registration,” in [*Proceedings of MICCAI 2005*], **LNCS 3750**, pp.543–550 (2005).
- [9] Helferty, J. P. and Higgins, W. E., “Technique for registering 3d virtual ct images to endoscopic video,” in [*Proceedings of ICIP (International Conference on Image Processing)*], 893–896 (2001).
- [10] Chung, A. J., Deligianni, F., Shah, P., Wells, A., and Yang, G. Z., “Patient-specific bronchoscopy visualization through brdf estimation and disocclusion correction,” *IEEE Transactions on Medical Imaging* **25**(4), 503–513 (2006).
- [11] Deguchi, D., Mori, K., Feuerstein, M., Kitasaka, T., Maurer Jr., C. R., Suenaga, Y., Takabatake, H., Mori, M., and Natori, H., “Selective image similarity measure for bronchoscope tracking based on image registration,” *Medical Image Analysis* **13**(4), 621–633 (2009).
- [12] Solomon, S. B., P. White, J., Wiener, C. M., Orens, J. B., and Wang, K. P., “Three-dimensional ct-guided bronchoscopy with a real-time electromagnetic position sensor: a comparison of two image registration methods,” *Chest* **118**(6), 1783–1787 (2000).
- [13] Deguchi, D., Ishitani, K., Kitasaka, T., Mori, K., Suenaga, Y., , Takabatake, H., Mori, M., and Natori, H., “A method for bronchoscope tracking using position sensor without fiducial markers,” in [*SPIE Medical Imaging*], **6511**, 65110N (2007).
- [14] Wengert, C., Reeff, M., Cattin, P. C., and Szekely, G., “Fully automatic endoscope calibration for intraoperative use,” in [*Bildverarbeitung fur die Medizin, Springer-Verlag*], **19-21**, 419–423 (2006).
- [15] Zhang, Z., “A flexible new technique for camera calibration,” *IEEE Transactions on Pattern Analysis and Machine Intelligence* **22**(11), 1330–1334 (2000).
- [16] Tsai, R. Y. and Lenz, R. K., “A new technique for fully autonomous and efficient 3d robotics hand/eye calibration,” *IEEE Transactions on Robotics and Automation* **5**(3), 345–358 (1989).

- [17] Eggert, D., Lorusso, A., and Fisher, R., “Estimating 3-d rigid body transformations: a comparison of four major algorithms,” *Machine Vision and Applications* **9**(5-6), 272–290 (1997).
- [18] Becker, H. D., Herth, F., Ernst, A., and Schwarz, Y., “Bronchoscopic biopsy of peripheral lung lesions under electromagnetic guidance: a pilot study,” *Journal of Bronchology* **12**(1), 9 (2005).
- [19] Soper, T. D., Haynor, D. R., Glenny, R. W., and Seibel, E. J., “A model of respiratory airway motion for real-time tracking of an ultrathin bronchoscope,” in [*SPIE Medical Imaging*], **6511**, 65110M (2007).